Meteorological Response of Kamchatka Seismicity

Alexander Schekotov, Karina Borovleva, Vyacheslav Pilipenko, Danila Chebrov, and Masashi Hayakawa

Alexander Schekotov Deceased April 3, 2023

Abstract We have carried out a preliminary study of the relationship between local seismicity and the behavior of atmospheric temperature and humidity based on data from the local seismic catalog and archival data from the Karimshina observatory in Kamchatka. The chemical potential of water vapor molecules contained in the surface layer of the atmosphere was used as a measure of the impact of seismic processes on the atmosphere. Following the accepted terminology, we call it the atmospheric chemical potential (*ACP*), which is calculated from the air temperature and humidity. *ACP* supposedly increases in the process of air ionization by radon (Rn) which is released during the enhancement of seismic activity. It is assumed that Rn rises to the surface more intensively along seismic faults or volcanic fumaroles. Air ionization leads to a decrease in the air humidity and an increase in its temperature, and eventually results in an increase of *ACP*. We have subtracted the 30-day moving average of the *ACP* from its time variations to better reveal the ionization contribution. Thus, intervals of increased *ACP* were found in the temporal vicinity of earthquakes. The duration of these intervals ranged from a week to a month or more. The maximum response of the atmosphere to deep earthquakes is weaker and shifts closer to and beyond the date of a seismic event. The effect was more evident when the wind was directed from an expected Rn release region towards the observatory. We have not

A. Schekotov · K. Borovleva · V. Pilipenko (✉)
Institute of Physics of the Earth, Russian Academy of Sciences (IPE RAS), B. Gruzinskaya 10, Moscow 123242, Russia
e-mail: pilipenko_va@mail.ru; space.soliton@gmail.com

D. Chebrov
Kamchatka Branch of Geophysical Survey of Russian Academy of Sciences (KB GS RAS), Petropavlovsk-Kamchatski, Russia

M. Hayakawa
Hayakawa Institute of Seismo Electromagnetics, Co. Ltd. (Hi-SEM), University of Electro-Communications, 1-1-1 Kojima-Cho, Chofu Tokyo 182-0026, Japan

Advanced Wireless and Communications Research Center (AWCC), University of Electro-Communications, 1-5-1 Chofugaoka, Chofu Tokyo 182-8585, Japan

A. Kosterov et al. (eds.), *Problems of Geocosmos—2022*, Springer Proceedings in Earth and Environmental Sciences, https://doi.org/10.1007/978-3-031-40728-4_17

found a relationship between the magnitude of earthquakes and the magnitude of the *ACP* response. The reliability of these conclusions as well as the possibility of using the meteorological methods for earthquake prediction will be further examined.

Keywords Seismogenic meteorological phenomena · Radon Emanation · Air ionization · Atmospheric chemical potential · Earthquake preparation process · Earthquake prediction

1 Introduction

Despite the promising prospects for predicting earthquakes (EQs) based on electromagnetic phenomena [1–3], they are difficult to implement in regions with a high population density and a high level of electromagnetic interference. That is why it is important to look for other types of phenomena associated with seismicity, but less sensitive to electromagnetic interference. In this study, we examine response of the atmospheric chemical potential (*ACP*) to Kamchatka EQs. It was suggested that an increase in *ACP* caused by ionization of the air by radon Rn which is released during the enhancement of seismic activity. It is assumed that Rn lifts to the surface through faults in the Earth's crust [4] or volcanic fumaroles. Ionization by Rn was considered as a key player in the lithosphere-atmosphere–ionosphere coupling process [5–11]. These studies and references in them indicated the possibility of using this phenomenon to predict EQs.

However, natural diurnal and seasonal fluctuations in atmospheric parameters, rainfall, snowstorms, and wind can prevent reliable detection of the seismic-associated meteorological phenomenon. This study provides examples of detecting an increase in *ACP* in the temporal neighborhood (from a few days to a few months) of EQs and illustrates the properties of the phenomenon. We also examine the influence of the wind direction and velocity on the visibility of the effect and try to find a relationship between the magnitude of EQs and that of the *ACP* response.

This paper is organized as follows. The collection of seismic and weather data and their processing are presented in Sect. 2, and observational results are shown in Sect. 3. Finally, in Sect. 4 we discuss observational results and make recommendations for future research.

2 Data, Physical Background, and Processing

We took EQ data from the local Kamchatka catalog (https://sdis.emsd.ru/info/earthquakes/catalogue.php). The meteorological data were obtained at the Karimshina Observatory (KRM) with geographic coordinates 52.8° N, 158.15° E.

The chemical potential of water vapor molecules contained in the near-surface layer of the atmosphere was suggested as a diagnostic parameter [8]. In classical

thermodynamics, the chemical potential for a mixture of gases is found from the relationship between the differentiation of internal energy U, entropy S, volume V, temperature T, gas pressure p, and the number of particles in the gas N_i:

$$\mathrm{dU} = \mathrm{TdS} - \mathrm{pdV} + \sum_{\mathrm{i}} \mu_{\mathrm{i}} \mathrm{dN_i} \tag{1}$$

where index i indicates the number of gas in the mixture. Hence it follows that

$$\mu_{\mathrm{k}} = \left(\frac{\mathrm{dU}}{\mathrm{dN_k}} \right)_{\mathrm{T,V,N_{i \neq k}}} \tag{2}$$

From the relationships (1, 2) a correction to the chemical potential of water vapor molecules can be obtained, which is the binding energy of water molecules with an ion to which it is connected via the hydration process [12]

$$\Delta \mathrm{U(eV)} = 5.8 \times 10^{-10} (20\mathrm{T} + 5463)^2 \ln \left(\frac{100}{Hum} \right) \tag{3}$$

Here T is air temperature in °C, and Hum is relative humidity in %. The authors [12] called ΔU the atmospheric chemical potential (ACP), and this notation is used in this work as well.

We analyze the relationship between the maximum daily values of ACP and seismicity. To do this, we use the maximum daily temperature $T_{\max}$ and minimum daily humidity $Hum_{\min}$. We then compare these values with the local seismicity, which is characterized by the local seismicity coefficient K_{LS}. This coefficient is proportional to the EQ energy and inversely proportional to the distance R (in km) to the epicenter [3]:

$$\mathrm{K_{LS}} = \frac{10^{0.75 \mathrm{M_L}}}{10(\mathrm{R} + 100)} \tag{4}$$

where M_L is the EQ local magnitude.

Previous experience [2, 7] has shown that meteorological phenomena caused by seismicity are rather short-lived—their duration is several days, whereas ordinary meteorological phenomena, as well as ACP, are subjected to seasonal variations. Therefore, to improve the detection of short-lived anomalies, we have subtracted the 30-day moving average from the original data. As a result, we have obtained the ACP variations $\delta(ACP)$, which are calculated as follows:

$$\delta(\mathrm{ACP})_{\mathrm{i}} = \mathrm{ACP_i} - \frac{1}{\mathrm{N}} \sum_{\mathrm{j}=i-N}^{\mathrm{j}=i-1} \mathrm{ACP_j} \tag{5}$$

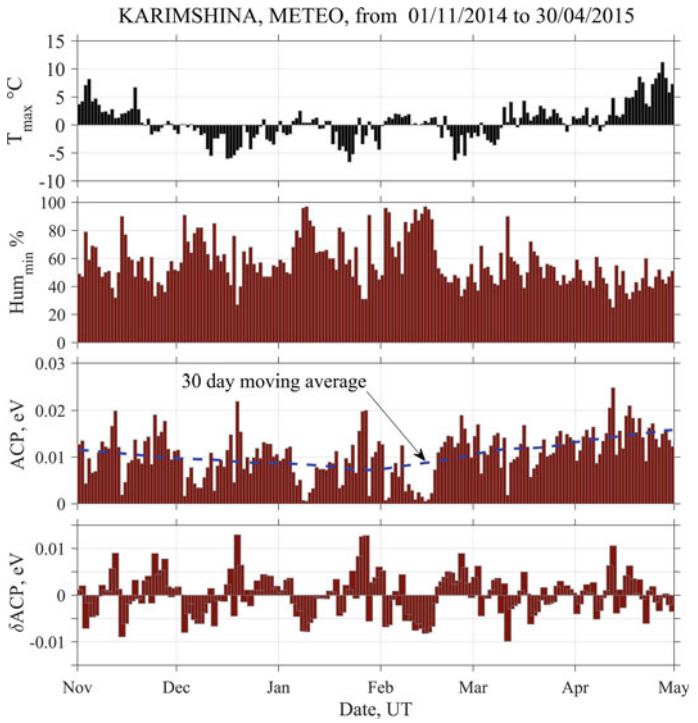

Fig. 1 The evolution of maximum daily temperature (upper panel), and minimum daily humidity (second panel). The third panel refers to the variations of *ACP* together with its moving average (dashed blue line), and the bottom panel refers to the detrended variations $\delta(ACP)$

Here *ACP* is the atmospheric chemical potential value for *i*-th date, and *N* is averaging interval equal to the number of preceding days.

Figure 1 shows an example of such calculations of the Karimshina data for the period of 6 months. Here, the evolution of maximum daily temperature $T_{\max}$ is depicted in the top panel, and the next panel dispalays the minimum daily humidity ($Hum_{\min}$). The third panel shows the evolution of *ACP* together with its 30-day moving average curve (blue dashed line). The bottom panel shows the detrended variations $\delta(ACP)$. Further, we will be interested only in its positive values $\delta(ACP)_{pos}$, which correspond to the process of condensation due to air ionization.

3 Results

Figure 2 illustrates the reaction of the local atmosphere to the seismicity of Kamchatka during half a year period from November 2014 to April 2015. The evolution of seismicity, maximum daily air temperature, and minimum humidity

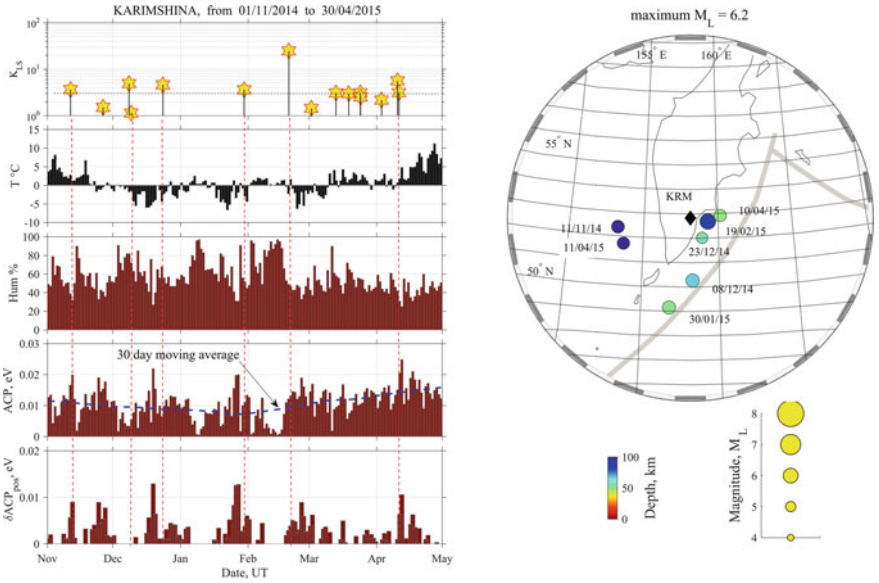

Fig. 2 Semi-annual evolution of meteorological parameters depending on seismicity. Evolution of seismicity is depicted in the top panel, temperature on second, and humidity in the third panel. Variations of *ACP* and it's running average are shown in the fourth panel. The $\delta(ACP)_{pos}$ variations are depicted in the bottom panel. Map of the region under study is shown on the right. The EQ epicenters are denoted by color circles. The colored bar below the map shows the corresponding EQ depth. The panel to the right with yellow circles reflects the correspondence between the diameter of the circles and local EQ magnitudes. Thick gray lines indicate the position of the Kuril-Kamchatka and Aleutian trenches

are presented in the first to third panels, respectively. Panel 4 shows the evolution of the *ACP* and its moving average. The positive variations of *ACP* relative to the moving average are displayed in the bottom panel. The figure reveals six intervals of increased *ACP*, and all of them are found to correspond to the time intervals with an increased seismic activity. A map of 800 km around the Karimshina observatory with the seven most significant EQs is shown on the right.

In Fig. 3 we compare the *ACP* and $\delta(ACP)_{pos}$ responses to a deep EQ (2015/10/16, $M_L = 5.9$, Depth = 295 km) and a relatively shallow EQ (2015/10/14, $M_L = 6.1$, Depth = 42 km). This comparison shows that there is delay in the $\delta(ACP)_{pos}$ response for a deep EQ as compared with that for a shallow EQ.

Figure 4 illustrates the effect of wind direction on the *ACP* variations. Here the presentation of panels is the same as before, except for the fourth panel which shows the evolution of the average daily wind direction and its speed. One can see a clear decrease or even disappearance of the $\delta(ACP)_{pos}$ variations when the wind is directed towards the EQ (wind direction of $0 \pm 45°$). This result also shows that the detection zone of meteorological seismogenic phenomena exceeds the dimensions of the EQ preparation zone calculated according to Dobrovolsky's relationship and equals in this case to ~280 km. This EQ occurred at a distance of ~ 420 km.

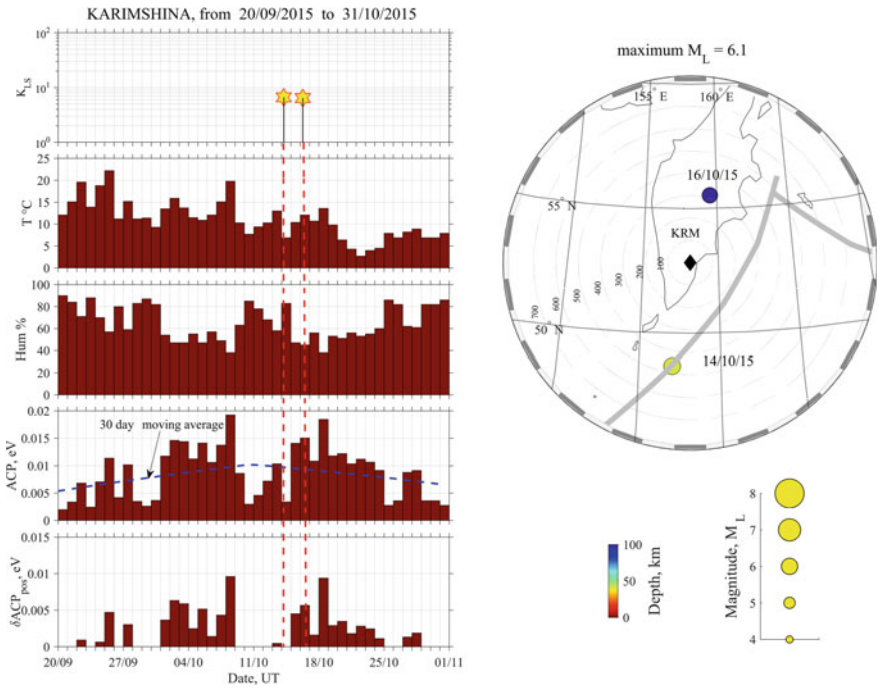

Fig. 3 Comparison of the $\delta(ACP)_{pos}$ responses for deep and shallow EQs. Here the format is the same as in Fig. 2. The $\delta(ACP)_{pos}$ response for the deep EQ is delayed relative to EQ date compared to the shallow one

Figure 5 illustrates the observational results for the Zhupanovsky EQ with $M_L = 7.1$ that occurred on 30 January 2016. Additionally, the figure presents the seismo-ionospheric ULF depression, that is the inverse magnitude of the band-integrated (0.01–0.03 Hz) spectral power [1–3]. The figure shows that a significant ULF power depression occurs simultaneously with the enhancement of $\delta(ACP)_{pos}$ about 80 days before the EQ. Both seismogenic phenomena occur almost simultaneously.

4 Discussion and Conclusion

Anomalous variations in meteorological conditions close to an epicenter zone before EQs were noticed even in early studies. For example, the Ashkhabad EQ of October 5, 1948 with $M = 7.3$ occurred after a long period of decrease in annual precipitation that had started in 1930 [13]. During 90 years of observation (1892–1981), the year of the EQ was the driest. No similar effect has been recorded at meteorological stations in other regions. The air temperature rose over a long period before 1948 and fell subsequently. Also, the warming that started about a year before Tashkent in 1984

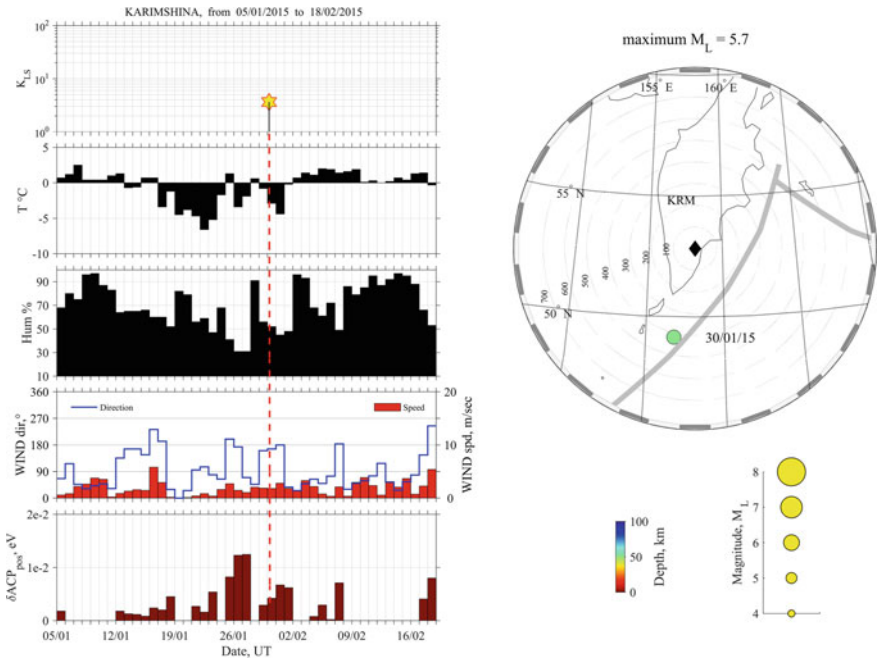

Fig. 4 The wind effect on the $\delta(ACP)_{pos}$ variations. Format is the same as Figs. 2 and 3, but the fourth panel shows the evolution of the average daily wind direction and its speed. Variations $\delta(ACP)_{pos}$ decreases when the wind is directed away from the observation point towards the epicenter (wind direction $0 \pm 45°$)

and Gazli in 1976 EQs were noticed. Many non-professional observers noticed that a peculiarity of periods preceding EQ was low cloudiness and fair weather.

Another indication on the influence of the seismic processes on the near-Earth atmosphere and meteorological processes was found upon investigation of the cloudiness in seismo-active regions with the use of Earth imagers from meteorological satellites [14]. Analysis of images from NOAA-11, -12 satellites showed that linearly extended clouds above Asia continent were associated with active tectonic faults. Mostly, cloud anomalies occurred at some distances from epicenters before and after EQ. Analysis of cloudiness at altitudes 0.5–6 km above Middle Asia from "Meteor" satellite showed either a formation of a cloud row or a sharp dissolvent of cloudiness above regional faults [15]. However, those early results did not get much attention, because of a lack of any reliable physical model during those times to interpret the meteorological observations. Nowadays, there appeared ever mounting number of evidences of a key role of radioactive emanations (e.g., Rn) in seismo-atmospheric coupling.

In this study, we have attempted to improve the detection of seismogenic atmospheric impact caused by the release of radon during the preparation process of EQs and tried to determine properties of this effect. As an impact parameter we

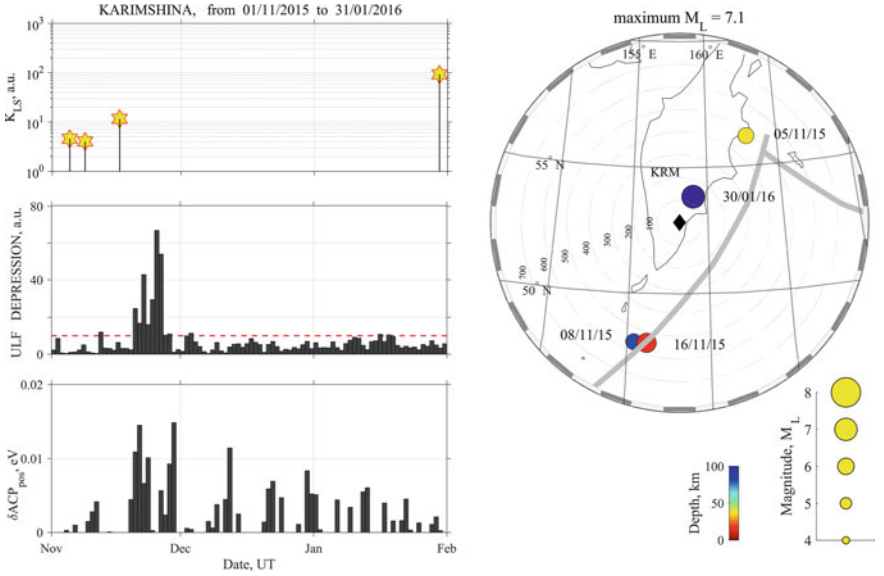

Fig. 5 Evolution of seismicity (upper panel), ULF seismo-ionospheric depression (middle panel), and $\delta(ACP)_{pos}$ variations (bottom panel) before the Zhupanovsky EQ with $M_L = 7.1$ and hypocenter depth 178 km

have used the potential of water vapor (*ACP*), calculated from the temperature and humidity of the air (Eq. 3). We have detrended variations relative to its 30-day moving average to remove background seasonal trend. The preliminary found properties of the meteorological response are listed below:

The removing of the *ACP* trend makes it much more reliable to detect its increase caused by a seismic activity;

- The increase in $\delta(ACP)_{pos}$ can outpace the date of a future EQ from several days to several weeks;
- The time of the $\delta(ACP)_{pos}$ increase may coincide with the seismo-ionospheric depression of the ULF power;
- A delay in the $\delta(ACP)_{pos}$ response for deep EQs with respect to shallow ones was found;
- The wind in the direction from the epicenter towards observation site increases the $\delta(ACP)_{pos}$ value and vice versa.

These conclusions were made thanks to the subtraction of the *ACP* trend, which has not been used by other authors [7] when processing meteorological data. As a result, this improvement in the analysis procedure enabled us to detect previously unknown atmospheric response properties. The search for seismic-related anomalies was also facilitated by the use of daily data of maximum temperature and minimum humidity, which made it possible to avoid interference in the form of diurnal fluctuations of these parameters.

We also concluded that the use of *ACP* is not very much justified for detecting seismogenic effects in the atmosphere, at least at Kamchatka. We believe that it is better to use variations in the inverse value of humidity (~1/*Hum*). First, as follows from the *ACP* expression (3), the effect of temperature on the result is insignificant. Moreover, seismogenic temperature variations are rare and small (see 2nd panel of Fig. 6). The main result of air ionization by radon emanation is a noticeable decrease in humidity, but its influence on *ACP* is weakened by the log-dependence in (3). Confirmations of this can be seen in Fig. 6.

Figure 6 displays a comparison of methods for detecting seismogenic effects on the atmosphere using the chemical potential (3) and just inverse humidity. Here, the top panel, as before, shows the evolution of local seismicity with K_{LS} index.

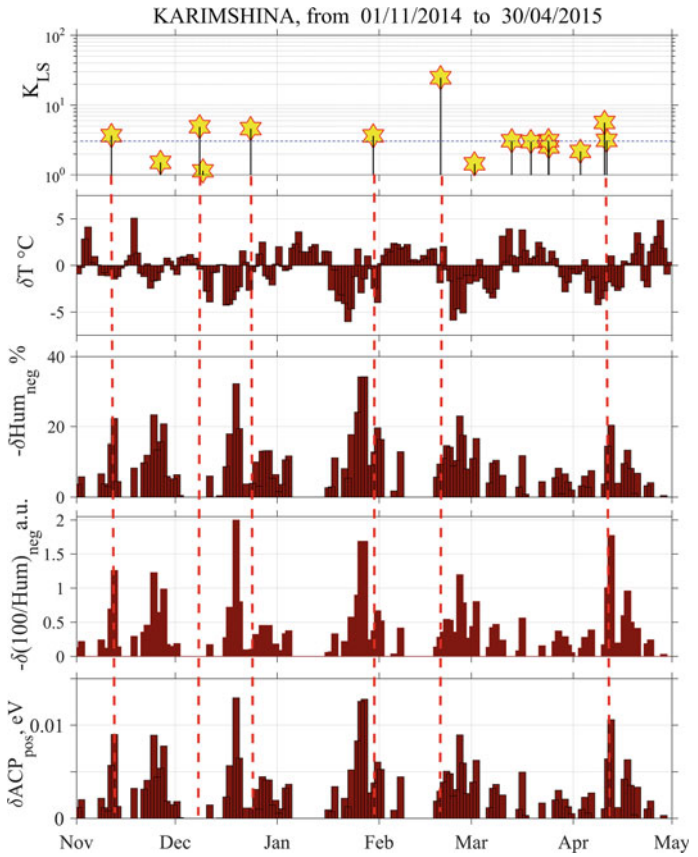

Fig. 6 Comparison of the use variations of *ACP* and inverse humidity for the detection of seismogenic weather phenomena. The top panel shows the evolution of seismicity, the second panel gives variations of maximum daily temperature, negative variations of humidity and its inverse values are shown on 3rd and 4th panels, and the bottom panel shows the evolution of the $\delta(ACP)_{pos}$ parameter

Variations of maximum daily air temperature are shown on 2nd panel. Negative variations of humidity and its inverse values are shown on 3rd and 4th panels. The bottom panel shows variations $\delta(ACP)_{pos}$. A comparison of the two lower panels indicates that the inverse magnitude of humidity is somewhat better than ACP for detecting air ionization. At this time interval, positive changes in temperature are observed, which do not coincide in time with a decrease in air humidity caused by radon ionization. Perhaps this is why the account of the influence of temperature hampers the detection of the phenomenon using *ACP*.

Despite the apparent correspondence of seismogenic responses to six most significant EQs, this result does not yet give us the right to assert the possibility of using this phenomenon for the EQ prediction. This interval was chosen when the electromagnetic precursors were slightly ahead of the events themselves. At the same time, Fig. 5 shows an example of an EQ, when the atmospheric and electromagnetic responses appear about 80 days before the EQ. To conclude that this phenomenon can be used for EQ prediction, it is highly required to examine statistical relationship between the atmospheric response and the parameters of the seismic processes that caused them. Furthermore, changes in humidity and air temperature caused by cyclones and typhoons mask seismic-induced increases in *ACP*. We will try to resolve these issues during further research. The direct comparison of variations of the meteorological parameters and Rn fluxes in boreholes and in the air will be provided elsewhere. However, according to some published measurements of Rn flux before EQs, its intensity is insufficient for the appearance of noticeable meteorological effects. Recently episodic measurements of Rn on local faults have begun, and we hope to see more encouraging results.

Acknowledgements We thank the whole staff of the Institute of Geophysical Survey RAS in Petropavlovsk-Kamchatsky for providing the data of weather, seismicity, and geomagnetic field. The seismic data used in the work were obtained with large-scale research facilities «Seismic infrasound array for monitoring Arctic cryolitozone and continuous seismic monitoring of the Russian Federation, neighboring territories and the world» (https://ckp-rf.ru/usu/507436/). We are also grateful to V. V. Surkov for comments and advices. This study was supported by grant 22-17-00125 from the Russian Science Foundation.

References

1. Hayakawa M., Schekotov A., Izutsu J., and Nickolaenko A.P. Seismogenic effects in ULF/ELF/VLF electromagnetic waves. International Journal of Electronics and Applied Research (IJEAR), 6, issue 2, 2019. https://doi.org/10.33665/IJEAR.2019.v06i02.001
2. Hayakawa M., Schekotov A., Izutsu J., Yang S.-S., Solovieva M., and Hobara Y. Multiparameter observations of seismogenic phenomena related to the Tokyo earthquake (M = 5.9) on 7 October 2021. Geosciences, 12, 265 (2022). https://doi.org/10.3390/geosciences12070265
3. Schekotov A., Chebrov D., Hayakawa M. et al. Short-term earthquake prediction in Kamchatka using low-frequency magnetic fields. Natural Hazards, 100, 735–755 (2020). https://doi.org/10.1007/s11069-019-03839-2

4. Kuntoro Y., et al. The correlation between radon emission concentration and subsurface geological condition. IOP Conference Series, Earth and Environmental Science, 132(1):012020, (2018). https://doi.org/10.1088/1755-1315/132/1/012020
5. Tronin A.A., Biagi P.F., Molchanov O.A., Khatkevich Y.M., and Gordeev E.I. Temperature variations related to earthquakes from simultaneous observation at the ground stations and by satellites in Kamchatka area. Physics and Chemistry of the Earth. Parts A/B/C, 29, 501–506 (2004). https://doi.org/10.1016/j.pce.2003.09.024
6. Giuliani G.G., Giuliani R., Totani G., Eusani G., and Totani F. Radon observations by gamma detectors PM-4 and PM-2 during the seismic period (January-April 2009) in L'Aquila Basin. Abstr. AGU Fall Meeting, December 14–18, 2009, San-Francisco, vol. 1: 03.
7. Pulinets S.A., Ouzounov D., Karelin A.V., Boyarchuk K.A., and Pokhmelnykh L.A. The physical nature of thermal anomalies observed before strong earthquakes. Physics and Chemistry of the Earth, Parts A/B/C, 31, 143–153 (2006). https://doi.org/10.1016/j.pce.2006.02.042
8. Pulinets S., and Ouzounov D. Lithosphere-Atmosphere-Ionosphere Coupling (LAIC) model – a unified concept for earthquake precursors validation. J. Asian Earth Sci, 41, 371–382 (2011). https://doi.org/10.1016/j.jseaes.2010.03.005
9. Pulinets S.A., Ouzounov D.P., Karelin A.V., and Davidenko D.V. Physical bases of the generation of short-term earthquake precursors: A complex model of ionization-induced geophysical processes in the lithosphere-atmosphere-ionosphere-magnetosphere system. Geomagn. Aeron., 55, 521–538 (2015). https://doi.org/10.1134/S0016793215040131
10. Pulinets S., Tsidilina M., Ouzounov D., and Davidenko D. From Hector Mine M7.1 to Ridgecrest M7.1 earthquake. A look from a 20-year perspective, Atmosphere, 12, 262 (2021). https://doi.org/10.3390/atmos12020262
11. Schekotov A., Hayakawa M., and Potirakis S.M. Does air ionization by radon cause low-frequency atmospheric electromagnetic earthquake precursors? Natural Hazards, 106, 701–714 (2021). https://doi.org/10.1007/s11069-020-04487-7
12. Boyarchuk K. A., Karelin A. V., Shirokov R. V. Baseline model of kinetics of ionized atmosphere. FSUE 'NPP VNIIEM', 204 p. 2006 (in Russian)
13. Milkis M.R. Meteorological precursors of strong earthquakes. Physics of the Solid Earth (Fizika Zemli), No. 3, 36–47, 1986.
14. Morozova L.I. Cloud indicators of the Earth crust geodynamics. Physics of the Solid Earth (Fizika Zemli), No. 10, 108–112, 1993.
15. Morozova L.I. Features of atmo-lithospheric relationships during periods of strong Asian earthquakes. Physics of the Solid Earth (Fizika Zemli), No. 5, 63–68, 1996.